JOC The Journal of Organic Chemistry

Article

pubs.acs.org/joc

A Selective, Sensitive, Colorimetric, and Fluorescence Probe for Relay Recognition of Fluoride and Cu(II) Ions with "Off−On−Off" Switching in Ethanol−Water Solution

Yu Peng,* Yu-Man Dong, Ming Dong, and Ya-Wen Wang*

State Key Laboratory of Applied Organic Chemistry, Key Laboratory of Nonferrous Metals Chemistry and Resources Utilization of Gansu Province and College of Chemistry and Chemical Engineering, Lanzhou University, Lanzhou 730000, People's Republic of China

Supporting Information

ABSTRACT: Anion to cation relay recognition was designed and realized for the first time with sequence specificity ($F^- \rightarrow Cu^{2+}$) via a fluorescence "off−on−off" mechanism. Probe **1** was a highly selective, sensitive, and turn-on chemodosimeter for F^- through a specific cyclization reaction triggered by the strong affinity of fluoride toward silicon with a significant change of fluorescence color in both ethanol and ethanol−water (1:1, v/v) solution. Fluorescence enhancement factors were dramatic: 833-fold in ethanol and 164-fold in ethanol−water (1:1, v/v) solution, respectively. The in situ system generated from the sensing of F^- showed good relay recognition ability for Cu^{2+} via fast fluorescence quenching by the formation of a 1:1 complex in ethanol−water (1:1, v/v) solution. The isolated pure compound **2** also exhibited high selectivity toward Cu^{2+} in PBS buffer (pH = 7.0) solution. The origin of this sequence specificity of fluorescence recognition was disclosed through the crystal or optimized structures and DFT calculations of corresponding compounds.

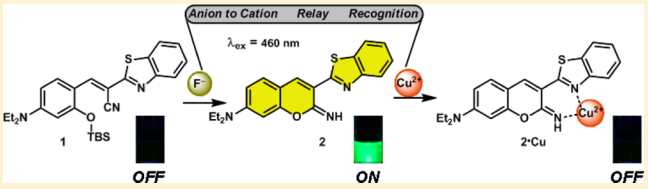

INTRODUCTION

Bifunctional probes, which refer to those based on a single host that can independently recognize two guest species with distinct spectra responses by the same or different channels, have already emerged and have gradually become a new research focus in the field of fluorescence sensors.[1] Recently, we have also reported two bifunctional probes that include combinations of Hg^{2+}/Au^{3+} and Al^{3+}/H^+.[2] Alternatively, we proposed a *relay recognition* strategy as a new pathway to dual-analyte fluorescent probes, which has been preliminarily demonstrated in the anion relay recognition (ARR) from F^- to CN^- based on the chemodosimeter approach associated with 1,1′-binaphthyl fluorophores (Scheme 1, top).[3] However, this relay probe has some significant drawbacks such as the extent of fluorescence enhancement, organic solvent media, UV light excitation, low sensitivity, etc. Herein, we disclose anion to cation relay recognition (ACRR) of F^- and Cu^{2+} based on the sequential chemodosimeter and chemosensor approaches (Scheme 1, bottom), which demonstrates significant improvement of fluorescence performance due to the formation of iminocoumarin−benzothiazole. Notably, the present fluorescence off-on-off switching is also quite different from our previous on-off-on switching in the CN^- to Au^{3+} relay probe[4] that involved a reversible process instead of the forward process used here.

RESULTS AND DISCUSSION

Design and Synthesis of Probe 1. Excessive ingestion of fluoride can result in fluorosis,[5] urolithiasis, or even cancer. Thus, recognition and sensing of F^- has received considerable attention recently.[6] Compared to the traditional chemosensor, the alternative chemodosimeter approach based on an irreversible specific chemical reaction has emerged as an active research area with significant importance recently.[7] Some recent chemodosimeters, utilizing desilylation reaction based on high affinity between silicon and fluoride ions,[8] have been developed successfully. However, most of these examples can only be operated in organic solvents[9] and are largely limited in practical application. To this end, design of new F^- probes with good performance in aqueous solution[10] by means of the desilylation reaction is still high desirable for potential biological applications.

We designed a colorimetric and turn-on chemodosimeter (**1**) for the rapid and highly selective detection of F^- with significant improvements to our latest, relatively inferior fluoride probe.[3] As shown in Scheme 2, fluoride triggers Si−O bond cleavage of probe **1**, and subsequent intramolecular nucleophilic attack of the generated phenolate on the *α,β*-unsaturated nitrile moiety by 1,2-addition and in 6-*exo*-*dig* fashion produces imine anion intermediate. This transient species quickly abstracts a proton from the solvent and

Received: July 26, 2012
Published: September 24, 2012

dx.doi.org/10.1021/jo301548v | J. Org. Chem. 2012, 77, 9072−9080

Scheme 1. Relay Recognition Strategy

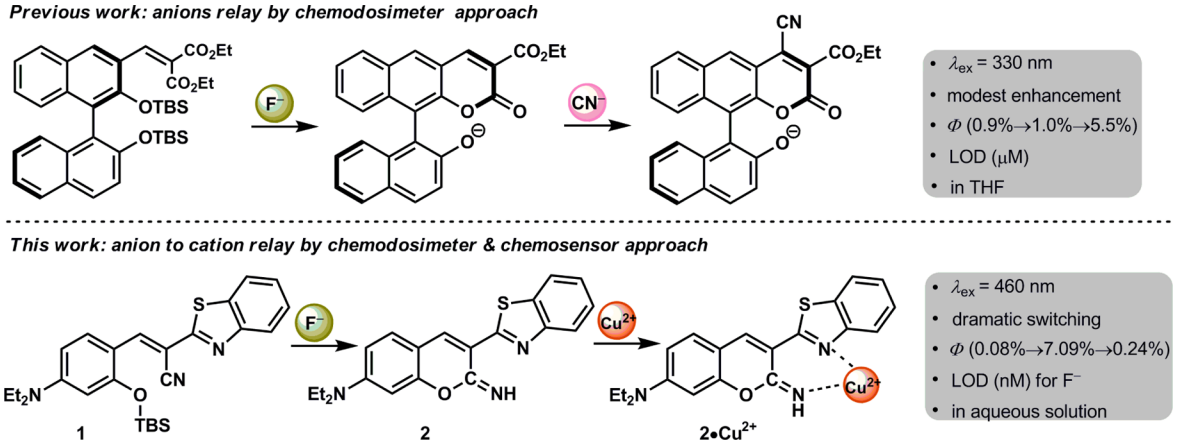

Scheme 2. Mechanism of Sensing Fluoride

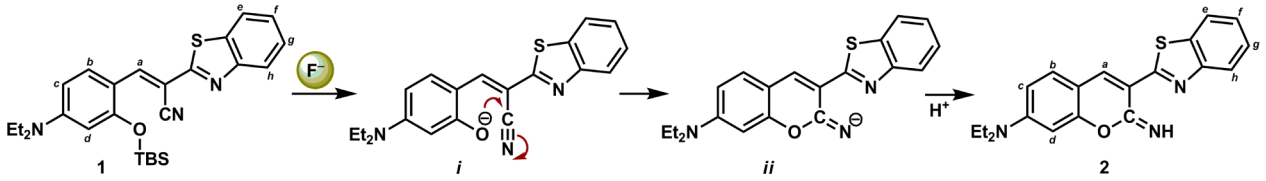

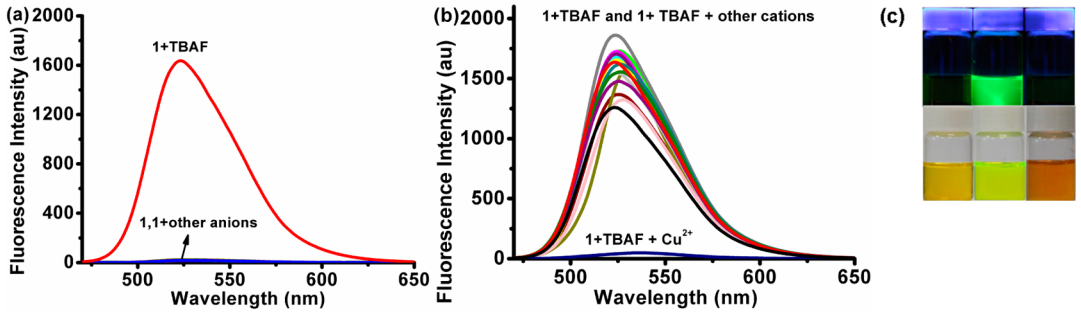

Figure 1. (a) Fluorescence responses of **1** (25.0 μM) with various anions (125.0 μM) in ethanol–water (v/v = 1:1) solution (λ_{ex} = 460 nm). (b) Fluorescence spectral changes of **1** + TBAF (25.0 μM + 125.0 μM) with various metal ions (125.0 μM) in ethanol–water (v/v = 1:1) solution (λ_{ex} = 460 nm). (c) Fluorescence change (top) and color change (bottom) of **1** (25.0 μM). From left to right: **1** only, F^- (1.0 equiv), F^- (1.0 equiv) + Cu^{2+} (1.0 equiv). All the images were obtained after 3 min upon the addition of ions.

eventually leads to the cyclization product iminocoumarin–benzothiazole **2**, which is responsible for the dramatic fluorescence enhancement. Notably, this cascade[11] to **2** is distinctively different from previous simple deprotection of *O*-silyl ethers[9b–g,10b–f] or desilylation followed by fragmentation.[10a,g] The designed chemodosimeter **1** was easily prepared by silylation of the free phenol hydroxyl group of 4-(diethylamino)salicylaldehyde with *tert*-butyldimethylsilyl chloride (TBSCl) and subsequent Knoevenagel condensation[12] with 2-benzothiazoleacetonitrile (see Scheme 3 in Experimental Section for details). The structure of **1** was identified by ^{1}H and ^{13}C NMR, IR, ESI-MS, HRMS (Figures S4–S8, Supporting Information), and X-ray crystal structure analysis (Figures 7 and S39, Supporting Information).

Fluorescence Responses of 1 with Relay Recognition of F^- and Cu^{2+}. Next, the fluorescence properties of **1** were studied. To date, most of the current fluorescence chemodosimeters that respond to F^- utilizing the desilylation reaction need to be excited by UV light,[9a–c,f,g,10d–g] which would inflict damage upon intracellular processes. As shown in Figure 1a, **1** exhibits a weak emission band at about 523 nm when excited at 460 nm, which is in the range of visible light and is relatively rare in aqueous solution.[10a,c] Subsequently, F^-, Cl^-, Br^-, I^-, AcO^-, ClO_4^-, $CF_3SO_3^-$, NO_3^-, HSO_4^-, $H_2PO_4^-$, BF_4^-, N_3^-, CN^-, SCN^-, and OH^- (as the corresponding tetrabutylammonium salt, respectively) were used to measure the selectivity of probe **1** (25.0 μM) in ethanol–water (1:1, v/v), and fluorescence spectra were recorded after 3 min upon addition of 5.0 equiv of each of these anions. Compared to other anions examined, only F^- generated a remarkable fluorescence increase at 523 nm.

Copper is the third most abundant essential trace element in the human body, plays a critical role in many cellular processes, and is also required by the human nervous system.[13] However, high levels of copper ions may also lead to neurodegenerative diseases such as Alzheimer's and Wilson's diseases,[14] which probably result from the production of reactive oxygen species (ROS). Thus, the sensing and recognition of copper ions has attracted considerable attention in recent years and resulted in fruitful work.[15] Since the pioneering work of Czarnik and co-workers in the development of a chemodosimeter for Cu^{2+} that utilizes rhodamine-B hydrazide,[16a] related fluorescent probes

dx.doi.org/10.1021/jo301548v | J. Org. Chem. 2012, 77, 9072–9080

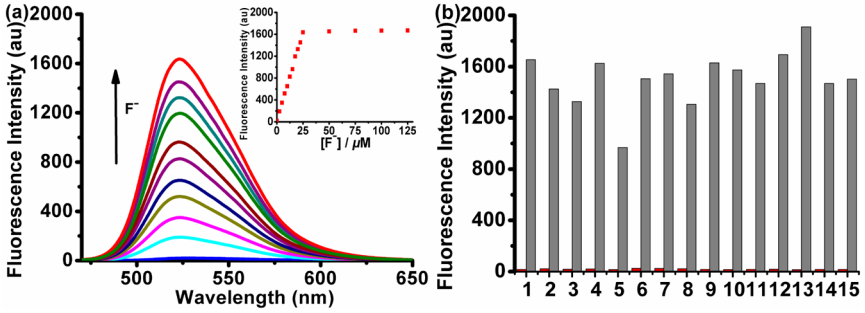

Figure 2. (a) Fluorescence spectra of **1** (25.0 μM) upon the addition of F^- in ethanol–water (v/v = 1:1) solution (λ_{ex} = 460 nm). [F^-] = 0, 2.5, 5.0, 7.5, 10.0, 12.5, 15.0, 17.5, 20.0, 22.5, 25.0, 50.0, 75.0, 100.0, 125.0 μM. Inset: Fluorescence intensity at 523 nm as a function of F^- concentration. (b) The selectivity of **1** (25.0 μM). The red bars represent the emission intensity of **1** in the presence of other anions (125.0 μM). The gray bars represent the emission intensity that occurs upon the subsequent addition of 25.0 μM F^- to the above solution. From 1 to 15: none, Cl^-, Br^-, I^-, AcO^-, ClO_4^-, $CF_3SO_3^-$, NO_3^-, HSO_4^-, $H_2PO_4^-$, BF_4^-, N_3^-, CN^-, SCN^-, and OH^- (λ_{em} = 523 nm).

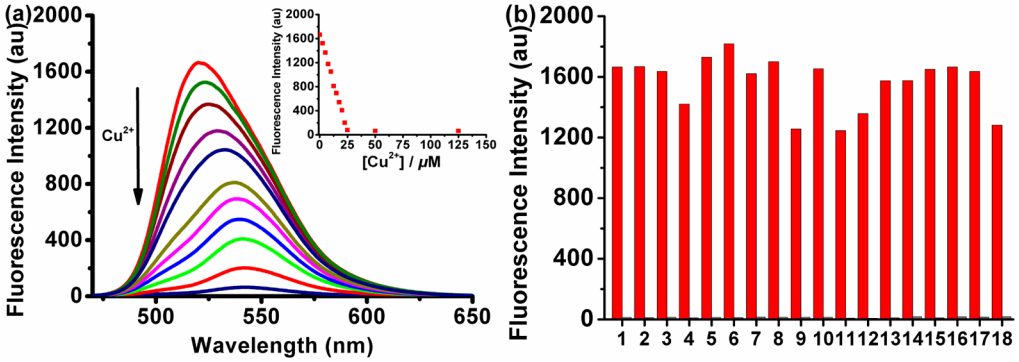

Figure 3. (a) Fluorescence spectra of **1** + TBAF (25.0 μM + 25.0 μM) upon the addition of Cu^{2+} in ethanol–water (v/v = 1:1) solution (λ_{ex} = 460 nm). [Cu^{2+}] = 0, 2.5, 5.0, 7.5, 10.0, 12.5, 15.0, 17.5, 20.0, 22.5, 25.0, 50.0, 125.0 μM. Inset: Fluorescence intensity as a function of F^- concentration. (b) The selectivity of **1** + TBAF (25.0 μM + 25.0 μM). The red bars represent the emission intensity of **1** + TBAF in the presence of other metal ions (125.0 μM) (λ_{em} = 523 nm). The gray bars represent the emission intensity that occurs upon the subsequent addition of 25.0 μM of Cu^{2+} to the above solution (λ_{em} = 544 nm). From 1 to 18: none, Na^+, Ca^{2+}, Mg^{2+}, Al^{3+}, Ba^{2+}, Zn^{2+}, Cd^{2+}, Co^{2+}, Hg^{2+}, Mn^{2+}, Ag^+, Fe^{2+}, Fe^{3+}, Pb^{2+}, Li^+, K^+, Ni^{2+}.

based on the spiro ring-opening of xanthene derivatives have been reported,[16b–f] including our recent contribution.[16e] Development of other effective Cu^{2+} fluorescent probes based on the chemosensor approach is still in high demand.

In the present work, iminocoumarin **2** generated in situ after recognition of F^- would be expected to serve as a relay probe for the sensing of some metal ions because several binding sites exist for coordination. Upon the addition of Cu^{2+} to the **1** + F^- system (**2**), fluorescence quench was indeed generated (Figure 1b). In contrast, no significant fluorescence changes were observed when other metal ions (including Na^+, Ca^{2+}, Mg^{2+}, Al^{3+}, Ba^{2+}, Zn^{2+}, Cd^{2+}, Co^{2+}, Hg^{2+}, Mn^{2+}, Ag^+, Fe^{2+}, Fe^{3+}, Pb^{2+}, Li^+, K^+, and Ni^{2+}) or anions (including Br^-, AcO^-, ClO_4^-, $CF_3SO_3^-$, NO_3^-, HSO_4^-, $H_2PO_4^-$, BF_4^-, N_3^-, CN^-, SCN^-, and OH^-) were added (Figures 1b and S13, Supporting Information). These results suggested that probe **1** displayed an excellent selectivity toward F^- in ethanol–water (1:1, v/v), and the resulting **1** + F^- system showed high selectivity for Cu^{2+} in the same media as well. To this end, the designed relay recognition of these two ions has been achieved with sequence specificity (F^-→Cu^{2+}) via a fluorescence "off–on–off" switching mechanism and provided a complementary sensing approach to previous bifunctional probes for F^- and Cu^{2+} ions.[1e,f]

It is noteworthy that the above relay recognition of two species (F^-→Cu^{2+}) can be defined as "anion→metal ion sequence" with a combination of the chemodosimeter and chemosensor approach that is very rare. In contrast, conventional demetalation (displacement) of the preassembled complex ("metal ion→anion recognition sequence")[17] generally features "on-off-on" switching based on chemosensor approach.

Relay Fluorescence Titrations with F^- and Cu^{2+}. The pH dependence of the fluorescence intensity change of **1** and the **1** + F^- system in the ethanol–water solution is shown in Figure S14 (Supporting Information). With the increase of the pH from 5.5 to 11.5, the fluorescence intensity of the **1** + F^- system increased significantly compared to the fluorescence intensity of **1**. Under extremely acidic or basic conditions, **1** cannot be used for the detection of F^-. Eventually ethanol–water (1:1, v/v, pH = 7.4) solution was used as an ideal media. The fluorescence titrations of F^- were also conducted using a 25.0 μM solution of **1** in ethanol–water (1:1, v/v) solution. Upon the addition of F^- to the solution, a significant increase (164-fold) in the fluorescence intensity at 523 nm was observed (Figure 2a) when excited at 460 nm. Further increase in the concentration of F^- (>25.0 μM) led to no further fluorescence increase (Figure 2a, inset), which clearly demonstrated a chemodosimeteric fluorescence change between F^- and probe **1**. The fluorescent quantum yield (Φ) of **1** also increased from 0.08% to 7.09% in the presence of F^- (1.0 equiv). The corresponding detection limit[18] was calculated to be 117.7 nM (2.24 ppb) (Figure S15, Supporting Information), which is much lower than the concentration allowed in drinking water

dx.doi.org/10.1021/jo301548v | J. Org. Chem. 2012, 77, 9072–9080

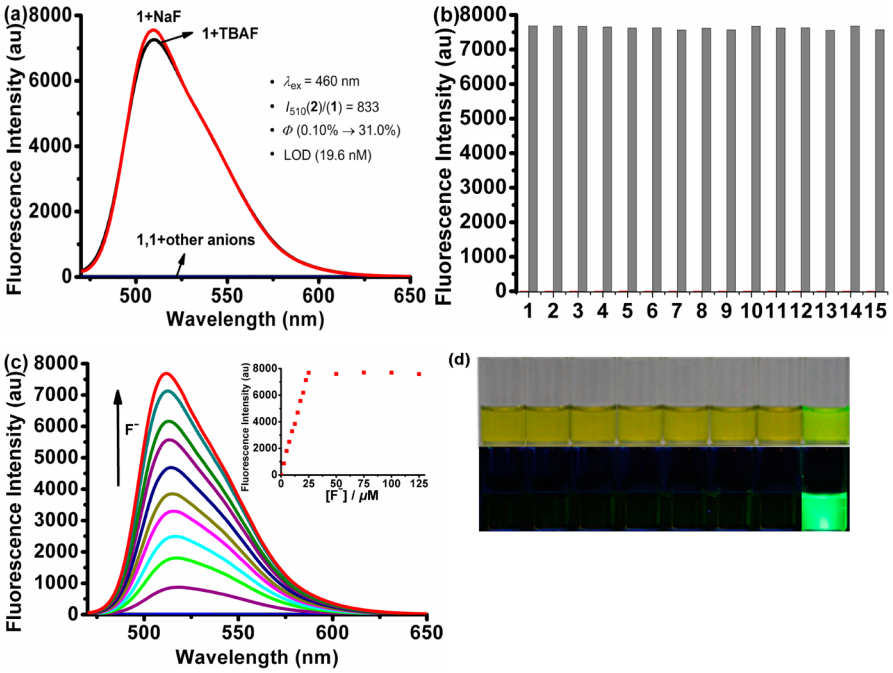

Figure 4. (a) Fluorescence responses of **1** (25.0 μM) with various anions (100.0 μM) in ethanol (λ_{ex} = 460 nm). (b) The selectivity of **1** (25.0 μM). The red bars represent the emission intensity of **1** in the presence of other anions (100.0 μM). The gray bars represent the emission intensity that occurs upon the subsequent addition of 25.0 μM of F^- to the above solution. From 1 to 15: none, Cl^-, Br^-, I^-, AcO^-, ClO_4^-, $CF_3SO_3^-$, NO_3^-, HSO_4^-, $H_2PO_4^-$, BF_4^-, N_3^-, CN^-, SCN^-, and OH^- (λ_{em} = 510 nm). (c) Fluorescence spectra of **1** (25.0 μM) upon the addition of F^- in ethanol. [F^-] = 0, 2.5, 5.0, 7.5, 10.0, 12.5, 15.0, 17.5, 20.0, 22.5, 25.0, 50.0, 75.0 μM. Inset: Fluorescence intensity at 510 nm as a function of F^- concentration. (d) Color change (top) and fluorescence change (bottom) of **1** ([**1**] = 25.0 μM, [F^-] = 50.0 μM, [other anions] = 100.0 μM). Left to right: **1** only, Cl^-, AcO^-, $CF_3SO_3^-$, NO_3^-, BF_4^-, CN^-, F^-.

according to the US EPA (1−4 ppm).[19] The kinetic behavior of F^- (250.0 μM) to probe **1** (25.0 μM) in ethanol−water (1:1, v/v) solution at 25 °C was measured (Figure S16, Supporting Information), and the observed rate constant was estimated to be k_{obs} = 5.84 × 10^{-3} s^{-1} by fitting the initial fluorescent intensity changes according to a pseudo-first-order kinetics equation. As shown in Figure 2b, all competitive anions caused no obvious changes, even at the higher concentration (125.0 μM); therefore, the **1** + F^- system was hardly affected by these coexistent ions. In addition, the fluorescence color changed from almost nonfluorescent to bright jade green with the addition of F^- (Figure 1c, top). The above results mean that **1** can function as a colorimetric and fluorescent probe for F^- via a fluorescence "turn-on" mechanism.

Then the generated **1** + F^- system was directly used to titrate Cu^{2+} without separation and purification. Upon the addition of Cu^{2+}, a significant decrease in the fluorescence intensity at 523 nm with a bathochromic shift to 544 nm was observed (Figure 3a). The total fluorescence intensity of the **1** + F^- system decreased to 1.9% when 1.0 equiv of Cu^{2+} was present. The fluorescence quench is due to LMCT between the **1** + F^- system (**2**) and Cu^{2+} by coordination, and this behavior has been further revealed by DFT calculations (vide infra, see also Figures 8, S42, S43, and S44, Supporting Information). Increase in the concentration of Cu^{2+} led to no further fluorescence quench (Figure 3a, inset), which demonstrated a 1:1 stoichiometry between the **1** + F^- system and Cu^{2+}. This ratio was also obtained by using Job's plot (Figures S17, Supporting Information). Moreover, the positive-ion ESI mass spectrum provides additional evidence for the formation of a 1:1 complex between the **1** + F^- system (**2**) and Cu^{2+} (Figure S18): a peak at m/z 511.0033 assigned to [**2** + Cu(II) + ClO_4]$^+$ is observed.[20] Based upon a 1:1 stoichiometry, the association constant K of the complex was then calculated to be 7.93 × 10^5 M^{-1} (Figure S19, Supporting Information).[21] The corresponding detection limit was calculated to be 1.79 μM (113.7 ppb) (Figure S20, Supporting Information). The fluorescent quantum yield (Φ) decreased from 7.09% to 0.24% in the presence of Cu^{2+} (1.0 equiv). As shown in Figure 3b, all competitive metal ions had no obvious interference with the detection of Cu^{2+} ion. The **1** + F^- system displayed high sensitivity for Cu^{2+} owing to the short response time (Figure S21, Supporting Information). These results clearly indicated that the **1** + F^- system (**2**) is useful for selectively sensing Cu^{2+} even under competition from other related metal ions, which would achieve the purpose of real-time monitoring. The fluorescence color changed from jade green to almost nonfluorescent (Figure 1c, top). All of these results suggested that relay **2** can also function as a fluorescent probe for Cu^{2+}.

Absorption Responses of 1 with Relay Recognition of F^- and Cu^{2+}. In the profile of UV−vis spectra of the probe **1** in ethanol−water (1:1, v/v) solution, an absorption peak emerged at about 460 nm, and its intensity slightly increased upon the addition of F^- (Figure S22, Supporting Information). However, only with the addition of Cu^{2+} to the **1** + F^- system was a new absorption peak observed, at about 503 nm, and its intensity gradually increased upon the addition of Cu^{2+} (Figures S22, S23, and S24, Supporting Information). Moreover, changes in the solution color from yellow to yellowish green and then to brownish yellow were observed by the naked eye upon the sequential addition of F^- and Cu^{2+} ions to probe **1** (Figure 1c, bottom). The absorption changes at 460 and 503 nm are in good agreement with these color changes. These results

dx.doi.org/10.1021/jo301548v | J. Org. Chem. 2012, 77, 9072−9080

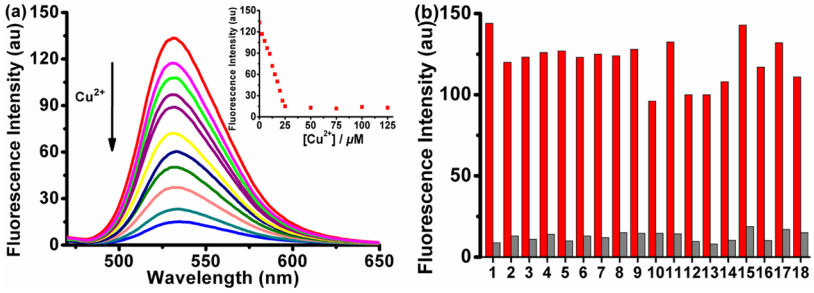

Figure 5. (a) Fluorescence spectra of **2** (25.0 μM) upon the addition of Cu^{2+} in PBS buffer (pH = 7.0) solution (λ_{ex} = 460 nm). [Cu^{2+}] = 0, 2.5, 5.0, 7.5, 10.0, 12.5, 15.0, 17.5, 20.0, 22.5, 25.0, 50.0, 75.0, 100.0, 125.0 μM. Inset: Fluorescence intensity at 533 nm as a function of F^- concentration. (b) The selectivity of **2** (25.0 μM). The red bars represent the emission intensity of **2** in the presence of other metal ions (125.0 μM). The gray bars represent the emission intensity that occurs upon the subsequent addition of 25.0 μM of Cu^{2+} to the above solution. From 1 to 18: none, Na^+, Ca^{2+}, Mg^{2+}, Al^{3+}, Ba^{2+}, Zn^{2+}, Cd^{2+}, Co^{2+}, Hg^{2+}, Mn^{2+}, Ag^+, Fe^{2+}, Fe^{3+}, Pb^{2+}, Li^+, K^+, Ni^{2+} (λ_{em} = 533 nm).

indicated that relay recognition of these two ions was realized through UV−vis spectroscopy as well.

Further Spectroscopic Investigation of 1 with F^- in Ethanol. Fluorescence properties of **1** and **1** + TBAF in a mixture of ethanol and water were further examined (Figure S25, Supporting Information). Compared to that in pure ethanol solution, the fluorescence of **1** + F^- exhibited a slight bathochromic shift, and its intensity was quenched to some extent in ethanol solution with different proportions of H_2O. The total fluorescence intensity of **1** increased to 584-, 459-, 223-, 212-, and 164-fold in ethanol with different proportions of water (10%, 20%, 30%, 40%, and 50%), respectively. Notablely, in pure ethanol solution the fluorescence enhancement factor at 510 nm was determined as a dramatic 833-fold, which is the highest value ever observed.[22] Eventually, the system of pure ethanol solution was selected to study the fluorescence response of **1** with F^- in detail. As shown in Figure 4a, compared to other anions examined, only F^- caused a remarkable fluorescence increase at 510 nm, and a similar result was observed by addition of a NaF[23] solution. All competitive anions had no obvious interference with the detection of F^- (Figure 4b). The fluorescence titration experiment shows that the addition of F^- to the solution resulted in a 833-fold fluorescence enhancement at 510 nm when excited at 460 nm, and further increase in the concentration of F^- (>25.0 μM) led to no further fluorescence increase (Figure 4c). The fluorescent quantum yield (Φ) of **1** increased significantly from 0.10% to 31.0% in the presence of F^- (1.0 equiv). The corresponding detection limit was calculated to be 19.6 nM (0.37 ppb) (Figure S26, Supporting Information). The observed rate constant at 25 °C was analogously estimated to be $k_{obs} = 7.09 \times 10^{-3}$ s^{-1} (Figure S27, Supporting Information). In addition, only the solution containing F^- showed the change in solution color from yellow to yellowish green, which was observed by the naked eye (Figure 4d, top). The significant change in fluorescence color from almost nonfluorescent to bright jade green was also demonstrated (Figure 4d, bottom).

There were no changes in the UV−vis spectra of probe **1** after addition of various anions in pure ethanol solution (Figure S28, Supporting Information). Upon the addition of F^-, the absorbance intensity at about 460 nm was slightly increased.

Further Spectroscopic Investigation of 2 with Cu^{2+} in PBS Buffer Solution. Finally, the fluorescence properties of the isolated pure compound **2** and **2** + Cu^{2+} were studied in detail. The fluorescence properties of **2** and **2** + Cu^{2+} in a mixture of ethanol and water were further examined (Figure S29, Supporting Information). Upon the addition of 1.0 equiv of Cu^{2+}, the total fluorescence intensity of **2** decreased to 1.9%, 2.2%, 3.2%, 4.5%, 8.3%, and 12.4% in ethanol with different proportions of water (50%, 60%, 70%, 80%, 90%, and 100%), respectively. Considering practical application, pure water solution was selected to study the fluorescence response of **2** with Cu^{2+} in detail. The pH effect on the fluorescence intensity is shown in Figure S30 (Supporting Information). The fluorescence intensity of **2** increased gradually in the pH range from 4.0 to 8.0, which may result from deprotonation of the protonated form (Et_2NH^+) of the diethylamino substituent. Upon the addition of Cu^{2+} to the solution of **2**, the fluorescence intensity quench may be due to the effective coordination between **2** and Cu^{2+}. Compared to the fluorescence intensity of **2**, the **2** + Cu^{2+} system quenched the fluorescence intensity severely between pH 7.0 and 8.0. In subsequent experiments, a pH 7.0 solution was used as an ideal media. Upon the addition of Cu^{2+} to the PBS buffer (pH = 7.0) solution, a decrease in the fluorescence intensity at 533 nm was observed when excited at 460 nm (Figure 5a). Minimum fluorescence intensity was shown when 1.0 equiv of Cu^{2+} was present, and the total fluorescence intensity of **2** decreased to 12.4%. A further increase in the concentration of Cu^{2+} led to no further fluorescence quench (Figure 5a, inset), which demonstrated a 1:1 stoichiometry between **2** and Cu^{2+}. The corresponding detection limit was calculated to be 1.15 μM (73.0 ppb) (Figure S31, Supporting Information), which is much lower than the concentration allowed in drinking water according to the US EPA (1.3 ppm). The fluorescent quantum yield (Φ) decreased from 1.77% to 0.20% in the presence of Cu^{2+} (1.0 equiv) in PBS buffer solution. Both Job's plot and Benesi−Hildbrand plot experiments also gave rise to the result indicating a 1:1 binding model between **2** and Cu^{2+} (Figures S32 and S33, Supporting Information). The association constant K of the complex was then calculated to be 4.01×10^6 M^{-1} by using the emission changes at 533 nm (Figure S33, Supporting Information). In contrast, no significant fluorescence changes were observed when other ions were added (Figures S34 and S35, Supporting Information). As shown in Figure 4b, all competitive metal ions had no obvious interference with the detection of Cu^{2+} ion. A short response time was observed in the **2** + Cu^{2+} system (Figure S36, Supporting Information). These results clearly indicated that **2** can serve as a relay probe to detect Cu^{2+} ion in aqueous solution even in pure water.

dx.doi.org/10.1021/jo301548v | J. Org. Chem. 2012, 77, 9072−9080

In the UV−vis spectra of **2** in PBS buffer solution, the absorbance at about 430 nm decreased with the enhancement of a new absorbance at about 485 nm only in the case of Cu^{2+} over other metal ions upon the addition of various metal ions (Figures S37 and S38, Supporting Information). Moreover, there was a good linearity between the ratios of the absorbances A_{430}/A_{485} and the concentration of Cu^{2+} in the range of 2.5 to 25.0 μM (Figure S38, inset, Supporting Information) and therefore allows quantitative detection of Cu^{2+} by absorption ratiometry. These results indicated that recognition of Cu^{2+} ions could be also well realized through UV−vis spectroscopy.

Rationalization of Relay Recognition of F^- and Cu^{2+}. To understand the proposed mechanism (Scheme 1 (bottom) and 2) further, $^1H/^{13}C$ NMR, IR, and ESI mass spectroscopy analysis experiments were subsequently carried out (Figures S9−S12, Supporting Information). ^1H NMR spectral analysis showed that the signal of the double bond proton H_a at around 8.48 ppm of **1** shifted downfield (8.92 ppm) after the addition of F^- and the signals of $H_{e,h}$, H_f, H_g, H_c, and H_d also shifted downfield to a different extent, while the signal of H_b shifted upfield, which suggested the formation of cyclization product **2** (Figures 6 and S9, Supporting Information). The broad band

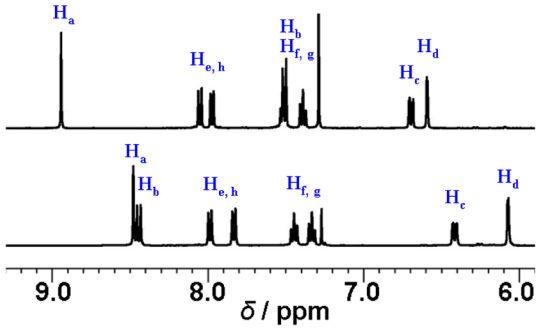

Figure 6. Partial ^1H NMR spectra (400 MHz) of **1** (bottom) and **2** (top) in $CDCl_3$.

around 3416 cm^{-1} in the IR spectrum corresponds to the N−H stretching frequency of **2** (Figure S11, Supporting Information). A major peak at m/z 350.3, corresponding to $[2 + H]^+$, is observed in the ESI mass spectrum (Figure S12, Supporting Information).

A single crystal of probe **1** was obtained from ethanol, and its structure (Figures 7 and S39, Supporting Information) shows

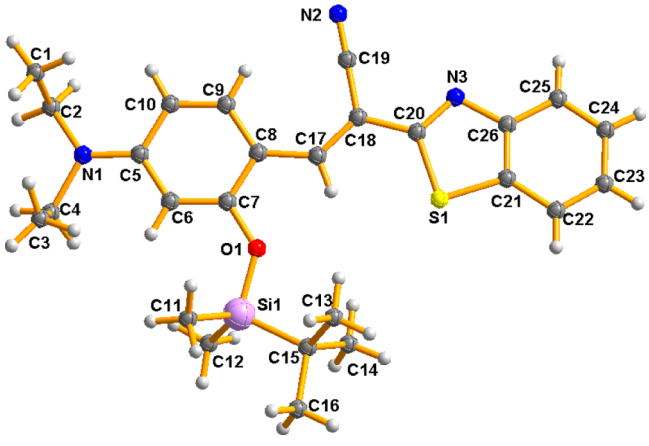

Figure 7. X-ray structure of **1**.

that the benzene ring and benzothiazole ring are not planar and their dihedral angle is about 11.8°. To further understand the relationship between the structural changes of **1** and **2** and the respective optical response to F^- and Cu^{2+}, we carried out density function theory (DFT) calculations with the B3LYP/6-31 G(d) basis set using the Gaussian 03 program. As displayed in Figures S40 and S41 (Supporting Information), the optimized structure of probe **1** has a dihedral angle of about 10.3° between the benzene ring and benzothiazole moiety, which is in good agreement with the corresponding crystallographic data of **1**, whereas the iminocoumarin and benzothiazole moieties of cyclization product **2** are essentially planar, with a dihedral angle of 0.8°, eventually resulting in the formation of delocalized π bonds. For probe **1**, both the HOMO and LUMO are mainly distributed at the benzene ring and benzothiazole moieties (Figure 8). By contrast, for the

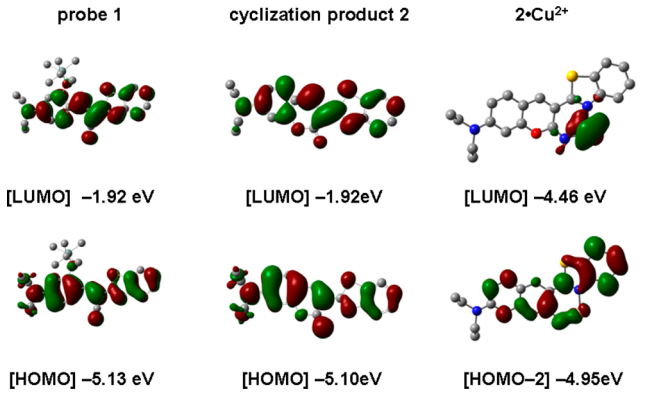

Figure 8. HOMO−LUMO energy levels and the molecular orbital plots of **1**, **2**, and **2**·Cu^{2+}.

cyclization product **2**, the HOMO and the LUMO are located over the whole molecule. These results indicate that **2** bears strong fluorescence character, which is the origin of the "turn-on" fluorescence response of **1** to F^- anions. Furthermore, the energy gap value between the HOMO and LUMO of **2** is similar to that of **1**, in good agreement with no obvious changes in the absorption spectra observed upon treatment of **1** with F^- anions. The optimized structure of **2**·Cu^{2+} complex shows that the Cu^{2+} ion binds to **2** at nitrogen atoms of the imino and benzothiazole groups, with Cu−N bond lengths 1.943 Å and 1.967 Å, respectively (Figure S42, Supporting Information). The Cu^{2+} ion may be chelated by the counteranion or solvent to satisfy the need for saturated coordination, and the iminocoumarin, benzothiazole, and Cu^{2+} ion are almost planar.[24] Considering the "soft" nature of the Cu^{2+} ion and the free rotation of the C−C single bond, the S center could also be involved in the complex, and the optimized structure of $[2\cdot Cu^{2+}]'$ complex was obtained accordingly (Figure S43, Supporting Information). In the **2**·Cu^{2+} complex, the electron density of HOMO−2 is mainly localized on the iminocoumarin and benzothiazole moieties while the electron density of LUMO is localized on the Cu^{2+} ion, which indicated a strong ligand-to-metal charge transfer (LMCT) process (Figure 8). A similar result was also observed in the $[2\cdot Cu^{2+}]'$ complex (Figure S44, Supporting Information), and the electron density change between HOMO−1 and LUMO was not sufficient to explain the LMCT process compared to that of the **2**·Cu^{2+} complex. Thus, **2** acts as a quenching fluorescent probe toward Cu^{2+} ion. The origin of the bathochromic shift in the

dx.doi.org/10.1021/jo301548v | J. Org. Chem. 2012, 77, 9072−9080

absorption spectra of the $2{\cdot}Cu^{2+}$ complex compared with that for **2** is attributed to LMCT between the **2** and Cu^{2+} by effective coordination.

CONCLUSION

We proposed a novel relay recognition concept from anion to cation and have realized unprecedented sensing of fluoride and copper(II) ions with sequence specificity via a fluorescence "off−on−off" mechanism. The fluorescence "turn-on"[7c] chemodosimeter **1** for F^- based on a specific cyclization reaction triggered by the strong affinity of fluoride toward silicon exhibits remarkable fluorescence enhancement, significant fluorescent quantum yield changes, high selectivity, and a very low detection limit, both in ethanol and its aqueous solution. The in situ prepared **1** + F^- system or pure **2** shows superior recognition ability for Cu^{2+} via fast fluorescence quenching by the formation of a 1:1 complex in ethanol−water (1:1, v/v) solution or PBS buffer (pH = 7.0) solution. Especially, iminocoumarin **2** is also potentially useful for quantitative determination of Cu^{2+} by absorption ratiometry in PBS buffer solution. Moreover, **1** and **2** can be excited by visible light and may be useful in potential biological applications. More applications of this efficient strategy might be found in extended occasions of this concept, such as with combinations of metal−metal ions and anion−neutral molecules.

EXPERIMENTAL SECTION

General Methods. Unless otherwise noted, materials were obtained from commercial suppliers and were used without further purification. Stock solutions (10 mM) of the tetrabutylammonium salts of F^-, Cl^-, Br^-, I^-, CN^-, AcO^-, ClO_4^-, $CF_3SO_3^-$, NO_3^-, HSO_4^-, $H_2PO_4^-$, BF_4^-, N_3^-, CN^-, and SCN_3^- in ethanol or deionized water, and NaF in deionized water, were prepared. Stock solutions (5 mM) of the perchlorate salts of Na^+, K^+, Li^+, Mg^{2+}, Ca^{2+}, Ba^{2+}, Al^{3+}, Mn^{2+}, Co^{2+}, Zn^{2+}, Cd^{2+}, Pb^{2+}, Fe^{2+}, Fe^{3+}, Cu^{2+}, Ag^+, and Hg^{2+} were prepared in deionized water. Stock solution of **1** (5 mM) or **2** (5 mM) was also prepared in ethanol. Test solutions were prepared by placing 10 μL of the probe stock solution into a test tube, diluting the solution to 2 mL with ethanol or ethanol−water (v/v = 1:1) or deionized water, and adding an appropriate aliquot of each anion stock. For all measurements, the fluorescence spectra were obtained by excitation at 460 nm. Both the excitation and emission slit widths were 2.5 nm. Fluorescence spectra were measured after 3 min upon the addition of anions. Fluorescent quantum yields were determined by standard methods, using fluorescein (Φ = 0.85 in 0.1 N NaOH) as a standard.[25]

Scheme 3. Synthesis of Probes 1 and 2

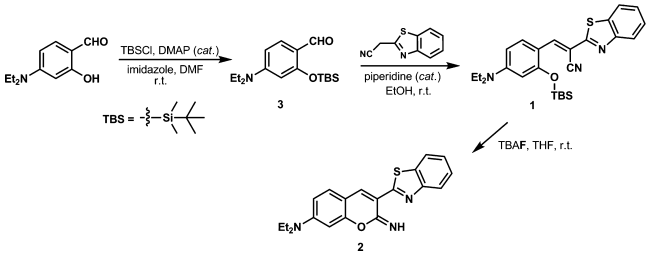

Synthesis and Characterization of Probe 1. To a solution of 4-(diethylamino)salicyaldehyde (1.93 g, 10 mmol) in dry DMF (50 mL) were added *tert*-butyldimethylsilyl chloride (TBSCl) (1.81 g, 12 mmol) and then imidazole (816 mg, 12 mmol) and DMAP (61 mg, 0.5 mmol). The mixture was stirred at room temperature for 15 h, quenched with water (30 mL), and extracted with ether (3 × 50 mL). The combined organic layers were washed with saturated NH_4Cl (50 mL), water (50 mL), and brine (50 mL) and then dried over $MgSO_4$. The solvent was removed under reduced pressure, and the residue was purified by column chromatography (petroleum ether/EtOAc = 50: 1) to give **3**[9a] as a white solid (1.35 g, 44%). ^{1}H NMR ($CDCl_3$, 400 MHz): δ 10.14 (s, 1H), 7.70 (d, J = 9.2 Hz, 1H), 6.33 (dd, J = 9.2, 2.0 Hz, 1H), 5.97 (d, J = 2.4 Hz, 1H), 3.39 (q, J = 7.2 Hz, 4H), 1.21 (t, J = 7.2 Hz, 6H), 1.03 (s, 9H), 0.28 (s, 6H) ppm; ^{13}C NMR ($CDCl_3$, 100 MHz): δ 187.4, 161.0, 153.5, 129.9, 116.4, 105.5, 100.5, 44.7 (2C), 25.7 (3C), 18.3, 12.5 (2C), −4.3 (2C) ppm; ESI−MS: m/z = 308.4 $[M + H]^+$. To a stirred solution of **3** (307 mg, 1 mmol) and 2-benzothiazoleacetonitrile (174 mg, 1 mmol) in ethanol (10 mL) at room temperature under argon was added one drop of piperidine. The reaction mixture was stirred at room temperature for 20 min. The solvent was evaporated under reduced pressure. The crude product was purified by column chromatography (petroleum ether/EtOAc = 30:1 → 10:1) on silica gel to afford compound **1** as a yellow solid (232 mg, 50%). Pure **1** was dissolved in EtOH, and single crystals were obtained by slow evaporation of solvent at room temperature after a few days. ^{1}H NMR ($CDCl_3$, 400 MHz): δ 8.48 (s, 1H), 8.45 (d, J = 9.2 Hz 1H), 8.00 (d, J = 8.4 Hz, 1H), 7.84 (d, J = 8.0 Hz, 1H), 7.45 (t, J = 8.0 Hz, 1H), 7.33 (t, J = 8.0 Hz, 1H), 6.42 (dd, J = 9.2, 2.4 Hz, 1H), 6.07 (d, J = 2.4 Hz, 1H), 3.41 (q, J = 7.2 Hz, 4H), 1.23 (t, J = 7.2 Hz, 6H), 1.11 (s, 9H), 0.30 (s, 6H); ^{13}C NMR ($CDCl_3$, 100 MHz): δ 165.7, 158.4, 153.9, 152.3, 141.8, 134.3, 130.2, 126.2, 124.8, 122.9, 121.2, 118.3, 112.1, 106.3, 100.8, 96.3, 44.8 (2C), 30.9, 25.8 (2C), 18.3, 12.6 (2C), −4.2 (2C) ppm; IR (film): ν_{max} = 3064, 2959, 2929, 2857, 2206 (−C≡N), 1608, 1561, 1511, 1404, 1352, 1281, 1246, 1114, 1076, 978, 891, 830, 783, 758 cm^{-1}; ESI−MS: m/z = 464.4 $[M + H]^+$; HRMS (ESI): calcd for $C_{26}H_{34}N_3OSSi^+$ $[M + H]^+$ 464.2186, found 464.2188.

Synthesis and Characterization of 2.[26] To a stirred solution of silyl ether **1** (50 mg, 0.108 mmol) in THF (10 mL) was added tetrabutylammonium fluoride in THF (1.0 M, 0.5 mL) at room temperature. The mixture was stirred for 3 h, and the solvent was evaporated under reduced pressure. The resulting crude residue was purified by flash column chromatography (10:1 → 1:1) on silica gel to afford compound **2** as a red solid (30 mg, 80%). ^{1}H NMR ($CDCl_3$, 400 MHz): δ (there is no signal of =N*H*) 8.92 (s, 1H), 8.03 (d, J = 8.4 Hz, 1H), 7.95 (d, J = 7.6 Hz, 1H), 7.50 (t, J = 8.0 Hz, 1H), 7.49 (d, J = 9.2 Hz, 1H), 7.37 (t, J = 8.0 Hz, 1H), 6.68 (dd, J = 9.2, 2.4 Hz, 1H), 6.57 (d, J = 2.4 Hz, 1H), 3.48 (q, J = 7.2 Hz, 4H), 1.26 (t, J = 7.2 Hz, 6H); ^{13}C NMR ($CDCl_3$, 100 MHz): δ 161.8, 161.0, 157.0, 152.6, 152.1, 142.0, 136.3, 130.7, 126.0, 124.4, 122.1, 121.5, 112.4, 109.9, 108.6, 96.9, 45.1 (2C), 12.5 (2C); IR (film): ν_{max} = 3416 (=NH), 3055, 2967, 2922, 1711, 1616, 1587, 1510, 1412, 1346, 1259, 1189, 1129, 1073, 1010, 936, 818, 756, 725, 674 cm^{-1}; ESI−MS: m/z = 350.3 $[M + H]^+$.

ASSOCIATED CONTENT

Supporting Information

Spectra data, cif file of the probe **1**, copies of ^{1}H/^{13}C NMR and ESI−MS. This material is available free of charge via the Internet at http://pubs.acs.org.

AUTHOR INFORMATION

Corresponding Author

*E-mail: pengyu@lzu.edu.cn; ywwang@lzu.edu.cn.

Notes

The authors declare no competing financial interest.

ACKNOWLEDGMENTS

This work was financially supported by the NSFC (nos. 21001058 and 21172096), the Scientific Research Foundation for the Returned Overseas Chinese Scholars, the Fundamental Research Funds for the Central Universities (lzujbky-2012-57), and the "111" Project of MoE.

DEDICATION

Dedicated to Professor A. P. de Silva (Queen's University, Northern Ireland) on the occasion of his 60th birthday.

REFERENCES

(1) For recent examples, see: (a) (NO and H_2O_2) Yuan, L.; Lin, W.; Xie, Y.; Chen, B.; Zhu, S. *J. Am. Chem. Soc.* **2012**, *134*, 1305. (b) (Hg^{2+} and Zn^{2+}) Satapathy, R.; Wu, Y.-H.; Lin, H.-C. *Org. Lett.* **2012**, *14*, 2564. (c) (F^- and CN^-) Guliyev, R.; Ozturk, S.; Sahin, E.; Akkaya, E. U. *Org. Lett.* **2012**, *14*, 1528. (d) (AcO^- and CN^-) Schmittel, M.; Qinghai, S. *Chem. Commun.* **2012**, *48*, 2707. (e) (Cu^{2+} and F^-) Bhalla, V.; Kumar, R.; Kumar, M.; Dhir, A. *Tetrahedron* **2007**, *63*, 11153. (f) (Cu^{2+} and F^-) Xu, Z.; Kim, S.; Kim, H. N.; Han, S. J.; Lee, C.; Kim, J. S.; Qian, X.; Yoon, J. *Tetrahedron Lett.* **2007**, *48*, 9151. For a review, see: (g) Lavigne, J. J.; Anslyn, E. V. *Angew. Chem., Int. Ed.* **2001**, *40*, 3118.

(2) (a) Dong, M.; Wang, Y.-W.; Peng, Y. *Org. Lett.* **2010**, *12*, 5310. (b) Sun, X.; Wang, Y.-W.; Peng, Y. *Org. Lett.* **2012**, *14*, 3420 and also see footnote 5 therein.

(3) Dong, M.; Peng, Y.; Dong, Y.-M.; Tang, N; Wang, Y.-W. *Org. Lett.* **2012**, *14*, 130.

(4) Dong, Y.-M.; Peng, Y.; Dong, M.; Wang, Y.-W. *J. Org. Chem.* **2011**, *76*, 6962.

(5) (a) Wiseman, A. *Handbook of Experimental Pharmacology XX/2*; Springer-Verlag: Berlin, 1970; Part 2, pp 48−97. (b) Weatherall, J. A. Pharmacology of Fluorides. In *Handbook of Experimental Pharmacology XX/1*; Springer-Verlag: Berlin, 1969; Part 1, pp 141−172. (c) Jagtap, S.; Kumar Yenkie, M.; Labhsetwar, N.; Rayalu, S. *Chem. Rev.* **2012**, *112*, 2454.

(6) These reviews are focused on the chemosensor approach; see: (a) Cametti, M.; Rissanen, K. *Chem. Commun.* **2009**, 2809. (b) Wade, C. R.; Broomsgrove, A. E. J.; Aldridge, S.; Gabbaï, F. P. *Chem. Rev.* **2010**, *110*, 3958.

(7) For recent reviews about the reaction-based sensing approach, see: (a) Cho, D.-G.; Sessler, J. L. *Chem. Soc. Rev.* **2009**, *38*, 1647. (b) Quang, D. T.; Kim, J. S. *Chem. Rev.* **2010**, *110*, 6280. (c) Jun, M. E.; Roy, B.; Ahn, K. H. *Chem. Commun.* **2011**, *47*, 7583. (d) Yang, Y.; Zhao, Q.; Feng, W.; Li, F. *Chem. Rev.* **2012**, *112*, DOI: 10.1021/cr2004103.

(8) Yamaguchi, S.; Akiyama, S.; Tamao, K. *J. Am. Chem. Soc.* **2000**, *122*, 6793.

(9) (a) Kim, T.-H.; Swager, T. M. *Angew. Chem., Int. Ed.* **2003**, *42*, 4803. (b) Jiang, X.; Vieweger, M. C.; Bollinger, J. C.; Dragnea, B.; Lee, D. *Org. Lett.* **2007**, *9*, 3579. (c) Bhalla, V.; Singh, H.; Kumar, M. *Org. Lett.* **2010**, *12*, 628. (d) Altan Bozdemir, O.; Sozmen, F.; Buyukcakir, O.; Guliyev, R.; Cakmak, Y.; Akkaya, E. U. *Org. Lett.* **2010**, *12*, 1400. (e) Cao, X.; Lin, W.; Yu, Q.; Wang, J. *Org. Lett.* **2011**, *13*, 6098. (f) Perry-Feigenbaum, R.; Sella, E.; Shabat, D. *Chem.−Eur. J.* **2011**, *17*, 12123. (g) Calderón-Ortiz, L. K.; Täuscher, E.; Bastos, E. L.; Görls, H.; Weiß, D.; Beckert, R. *Eur. J. Org. Chem.* **2012**, 2535.

(10) (a) (CH_3CN/H_2O = 1:1) Kim, S. Y.; Hong, J.-I. *Org. Lett.* **2007**, *9*, 3109. (b) (CH_3CN/H_2O = 7:3) Sokkalingam, P.; Lee, C.-H. *J. Org. Chem.* **2011**, *76*, 3820. (c) ($EtOH/H_2O$ = 3:7) Zhu, B.; Yuan, F.; Li, R.; Li, Y.; Wei, Q.; Ma, Z.; Du, B.; Zhang, X. *Chem. Commun.* **2011**, *47*, 7098. (d) (H_2O) Kim, S. Y.; Park, J.; Koh, M.; Park, S. B.; Hong, J.-I. *Chem. Commun.* **2009**, 4735. (e) (the micellar solution of $CTAB/THF/H_2O$) Hu, R.; Feng, J.; Hu, D.; Wang, S.; Li, S.; Li, Y.; Yang, G. *Angew. Chem., Int. Ed.* **2010**, *49*, 4915. (f) (DMF/H_2O = 9:1) Bao, Y.; Liu, B.; Wang, H.; Tian, J.; Bai, R. *Chem. Commun.* **2011**, *47*, 3957. (g) (CH_3CN/H_2O = 8:2) Zhang, J. F.; Lim, C. S.; Bhuniya, S.; Cho, B. R.; Kim, J. S. *Org. Lett.* **2011**, *13*, 1190.

(11) A similar two-step sequence (desilylation and cyclization to *lactone*, instead of *imine* in this work) had been reported by Swager and us; however, these probes could only work in pure organic solvents (THF and/or CH_2Cl_2) and showed limited fluorescence enhancement. For the details, see refs 9a and 3.

(12) Kürti, L.; Czakó, B. In *Strategic Applications of Named Reactions in Organic Synthesis: Background and Detailed Mechanisms*; Elsevier: Amsterdam, 2005; pp 242−243.

(13) (a) Uauy, R.; Olivares, M.; Gonzalez, M. *Am. J. Clin. Nutr.* **1998**, *67*, 952S. (b) Tapiero, H.; Townsend, D. M.; Tew, K. D. *Biomed. Pharmacother.* **2003**, *57*, 386. For a review, see: (c) Que, E. L.; Domaille, D. W.; Chang, C. J. *Chem. Rev.* **2008**, *108*, 1517.

(14) (a) Valentine, J. S.; Hart, P. J. *Proc. Natl. Acad. Sci. U.S.A.* **2003**, *100*, 3617. For a review, see: (b) Gaggelli, E.; Kozlowski, H.; Valensin, D.; Valensin, G. *Chem. Rev.* **2006**, *106*, 1995.

(15) (a) Jung, H. S.; Kwon, P. S.; Lee, J. W.; Kim, J. I.; Hong, C. S.; Kim, J. W.; Yan, S. H.; Lee, J. Y.; Lee, J. H.; Joo, T.; Kim, J. S. *J. Am. Chem. Soc.* **2009**, *131*, 2008. (b) Sheng, R.; Wang, P.; Gao, Y.; Wu, Y.; Liu, W.; Ma, J.; Li, H.; Wu, S. *Org. Lett.* **2008**, *10*, 5015. (c) Sanna, E.; Martínez, L.; Rotger, C.; Blasco, S.; González, J.; García-España, E.; Costa, A. *Org. Lett.* **2010**, *12*, 3840. (d) Ko, K. C.; Wu, J.-S.; Kim, H. J.; Kwon, P. S.; Kim, J. W.; Bartsch, R. A.; Lee, J. Y.; Kim, J. S. *Chem. Commun.* **2011**, *47*, 3165. (e) Li, P.; Duan, X.; Chen, Z.; Liu, Y.; Xie, T.; Fang, L.; Li, X.; Yin, M.; Tang, B. *Chem. Commun.* **2011**, *47*, 7755 . For a review, see: ref 7d and references cited therein.

(16) (a) Dujols, V.; Ford, F.; Czarnik, A. W. *J. Am. Chem. Soc.* **1997**, *119*, 7386. (b) Xiang, Y.; Tong, A.; Jin, P.; Ju, Y. *Org. Lett.* **2006**, *8*, 2863. (c) Zhou, Y.; Wang, F.; Kim, Y.; Kim, S.-J.; Yoon, J. *Org. Lett.* **2009**, *11*, 4442. (d) Zhang, J. F.; Zhou, Y.; Yoon, J.; Kim, Y.; Kim, S. J.; Kim, J. S. *Org. Lett.* **2010**, *12*, 3852. (e) Dong, M.; Ma, T.-H.; Zhang, A.-J.; Dong, Y.-M.; Wang, Y.-W.; Peng, Y. *Dyes Pigm.* **2010**, *87*, 164. For a review, see: (f) Chen, X.; Pradhan, T.; Wang, F.; Kim, J. S.; Yoon, J. *Chem. Rev.* **2012**, *112*, 1910 and references cited therein..

(17) For recent examples, see: (a) (Cu^{2+}→CN^-) Chung, S.-Y.; Nam, S.-W.; Lim, J.; Park, S.; Yoon, J. *Chem. Commun.* **2009**, 2866. (b) (Cu^{2+}→GMP) Amendola, V.; Bergamaschi, G.; Buttafava, A.; Fabbrizzi, L.; Monzani, E. *J. Am. Chem. Soc.* **2010**, *132*, 147. (c) (Ca^{2+}→F^-) Rochat, S.; Severin, K. *Chem. Commun.* **2011**, *47*, 4391. (d) (Ag^+→I^-) Wang, H.; Xue, L.; Jiang, H. *Org. Lett.* **2011**, *13*, 3844. (e) (Zn^{2+}→$H_2PO_4^-$) Ni, X.-l.; Zeng, X.; Redshaw, C.; Yamato, T. *J. Org. Chem.* **2011**, *76*, 5696. (f) (Cu^{2+}→PPi) Zhu, W.; Huang, X.; Guo, Z.; Wu, X.; Yu, H.; Tian, H. *Chem. Commun.* **2012**, *48*, 1784. (g) (La^{3+}→F^-) Sreenivasu Mummidivarapu, V. V.; Nehra, A.; Hinge, V. K.; Rao, C. P. *Org. Lett.* **2012**, *14*, 2968. For a review, see: (h) Nguyen, B. T.; Anslyn, E. V. *Coord. Chem. Rev.* **2006**, *250*, 3118−3127.

(18) For the method employed, see: Tong, C.; Xiang, G. *J. Lumin.* **2007**, *126*, 575−580 . See also ref 9e.

(19) http://water.epa.gov/drink/contaminants/basicinformation/fluoride.cfm.

(20) The Cu^{2+} ion may be chelated with counteranion or solvent molecules to satisfy the need for saturated coordination; for a similar hypothesis, see: Ko, K. C.; Wu, J.-S.; Kim, H. J.; Kwon, P. S.; Kim, J. W.; Bartsch, R. A.; Lee, J. Y.; Kim, J. S. *Chem. Commun.* **2011**, *47*, 3165.

(21) For the method employed, see: Benesi, H. A.; Hildebrand, J. H. *J. Am. Chem. Soc.* **1949**, *71*, 2703.

(22) To the best of our knowledge, the highest value reported to date is a ca. 500-fold intensity enhancement in ref 10a, where 1400 equiv of F^- was needed to reach saturation of the signals.

(23) In molecular and cell biology, NaF is known to influence various cell signaling processes; for the details, see: (a) Chen, T.-J.; Chen, T.-M.; Chen, C.-H.; Lai, Y.-K. *J. Cell. Biochem.* **1998**, *69*, 221. (b) Arhima, M. H.; Gulati, O. P.; Sharma, S. C. *Phytother. Res.* **2004**, *18*, 244.

(24) For the structure analysis about similar copper complex, see: Ahamed, B. N.; Ghosh, P. *Dalton Trans.* **2011**, *40*, 6411 and ref 20.

(25) Komatsu, K.; Urano, Y.; Kojima, H.; Nagano, T. *J. Am. Chem. Soc.* **2007**, *129*, 13447.

(26) This is a known compound; see: Kim, T.-I.; Kim, H.; Choi, Y.; Kim, Y. *Chem. Commun.* **2011**, *47*, 9825 and ref 25.

NOTE ADDED AFTER ASAP PUBLICATION

Since this published on October 2, 2012, the description of fluorescence switching in the Introduction and Results and Discussion has been corrected; it reposted on October 3, 2012.

dx.doi.org/10.1021/jo301548v | *J. Org. Chem.* 2012, 77, 9072−9080